Metrol. Meas. Syst., Vol. XXI (2014), No. 2, pp. 205–216.

METROLOGY AND MEASUREMENT SYSTEMS

Index 330930, ISSN 0860-8229

www.metrology.pg.gda.pl

POTENTIOMETRIC OXYGEN SENSOR WITH SOLID STATE REFERENCE ELECTRODE

Katarzyna Dunst, Grzegorz Jasinski, Piotr Jasinski

Gdansk University of Technology, Faculty of Electronics, Telecommunications and Informatics, ul. Narutowicza 11/12, 80-233 Gdansk, Poland (✉ pijas@eti.pg.gda.pl, +48 58 347 13 23)

Abstract

The concentration or the partial pressure of oxygen in an environment can be determined using different measuring principles. For high temperature measurements of oxygen, ceramic-based sensors are the most practical. They are simple in construction, exploration and maintenance. A typical oxygen potentiometric sensor consists of an oxygen ion conducting solid electrolyte and two electrodes deposited on the two sides of the electrolyte.

In this paper different structures of potentiometric oxygen sensors with a solid state reference electrode were fabricated and investigated. The fabricated structures consisted of oxygen ion conducting solid electrolyte from yttria stabilized zirconia, a sensing platinum electrode and nickel-nickel oxide reference electrode. The mixture of nickel-nickel oxide was selected as the reference electrode because it provides reliable electrochemical potential in contact with oxygen conducting electrolyte. To avoid oxidation of nickel the reference electrode is sealed from ambient and the mixture of nickel-nickel oxide was formed electrochemically from nickel oxide after sealing. The effectiveness of the sealing quality and the effectiveness of nickel–nickel oxide mixture formation was investigated by impedance spectroscopy.

Keywords: potentiometric, oxygen sensor, Nernstian behavior.

1. Introduction

Chemical sensors are used in a wide range of industries including steelmaking, heat treating, metal casting, glass, ceramic, pulp and paper, automotive and aerospace [1]. Monitoring and control of combustion–related emissions is a top priority in many industries. The major methods used to detect combustion gases fall short of practical applications for *in-situ* measurements in industrial environments involving high temperature and chemical contaminants. There is a continuing need for the development of fast, sensitive, rugged, reliable, and low-cost sensors for applications in harsh industrial environments [2, 3]. The real challenge is to develop highly sensitive and selective sensors with long-term stability in such aggressive environments [4].

Till today, the most popular are potentiometric electrochemical solid state sensors due to their widespread success in automotive industry. They operate in a very wide range of oxygen partial pressures, since their response is proportional to the logarithm of the oxygen pressure [5]. A typical oxygen potentiometric sensor consists of an oxygen ion conducting solid electrolyte and two electrodes deposited on the two sides of the electrolyte (see Fig. 1) [6]. One of these is a reference electrode and the other is a sensing electrode, which is exposed to the ambient with unknown (to be measured) oxygen partial pressure (concentration). The chemical potential of oxygen at the electrode/electrolyte interface is determined by the equilibrium at the triple phase boundary of gas, electrode and electrolyte. At the sensing electrode the chemical potential of oxygen depends on unknown oxygen partial pressure, while at the reference electrode it shall be fixed. As a result of oxygen chemical potential

Article history: received on Aug. 12, 2013; accepted on Feb. 08, 2014; available online on May. 15, 2014; DOI: 10.2478/mms-2014-0018.

difference between electrodes an electromotive force (EMF) is developed, which follows the Nernst equation [7].

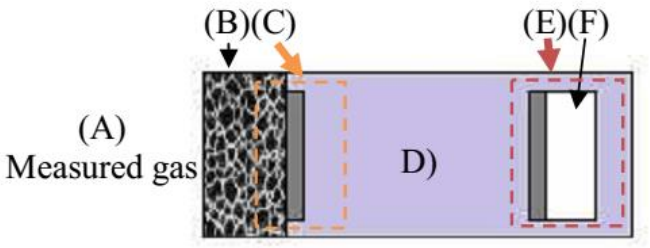

Fig. 1. Schematic structure of a potentiometric planar oxygen Lambda sensor. (A) - measured atmosphere, (B) - porous protective layer (it is optional), (C) - sensing electrode, (D) - O_2-ion-conductive ceramic electrolyte, (E) - reference electrode exposed to (F) ambient air atmosphere (adopted from [6]).

The oxygen chemical potential of the reference electrode can be fixed by known oxygen partial pressure (gaseous reference electrode) or by a mixture of the transition metal and its oxide (solid reference electrode) [6]. In case of the sensor with solid reference electrode the solid reference provides the equilibrium of the oxygen partial pressure at the operating temperature [8], so the chemical potential of oxygen at the reference electrode is formed in a similar matter as with gaseous reference electrode. The binary mixture systems used as solid reference electrodes have been reviewed in detail by Maskell et al. [9, 10].

The gaseous reference electrode is utilized very frequently in oxygen sensors. For example, in a Lambda sensor used widely for combustion control, the ambient air is provided from outside of the combustion environment to a reference electrode [7]. However, in some cases it is unfeasible to use sensors with a gaseous reference electrode. Sensors with a solid reference electrode are still at the stage of laboratory development. The difficulty in the sensor design is related to sealing of the reference electrode from the ambient gas against physical leakage of oxygen, which would affect the chemical potential of oxygen at the reference electrode [11]. However, proper isolation and sealing of the solid reference electrode under high temperature conditions would allow elimination of the gaseous reference required by commercial oxygen sensors [8]. This offers a great advantage in the microfabrication of the sensor [6]. Frequently, the process for developing this type of sensors requires different techniques like tape casting, screen printing, piling up substrates, or ceramic sintering. The structural and electrochemical properties of those devices are extremely depending on the processing conditions of these techniques [12].

In this paper a description of the fabrication process of the potentiometric oxygen sensors and results of their investigation are presented. The fabricated structures consisted of oxygen ion conducting solid electrolyte from yttria stabilized zirconia, a sensing platinum electrode and nickel-nickel oxide reference electrode. The mixture of nickel-nickel oxide was selected as the reference electrode because it provides a reliable electrochemical potential in contact with oxygen conducting electrolyte. One may be aware that there is the danger of alloy formation between Ni and inner Pt electrode at relatively low temperatures (around 700 ºC), which may lead to instability in sensor response [8]. However, the experimental studies have not confirmed this as a major issue [13]. To avoid oxidation of nickel, the reference electrode was sealed from the environment and the mixture of nickel-nickel oxide was formed electrochemically from nickel oxide after sealing. To the best of our knowledge, impedance

spectroscopy was employed for the first time to investigate the effectiveness of sealing of the reference electrode.

2. Theoretical considerations

For a sensor with a solid reference electrode, the following equation can be used to calculate an electromotive force *EMF* (1):

$$EMF = \frac{\Delta G}{zF} + \frac{RT}{zF} \ln p_{O_2}, \tag{1}$$

where F is the Faraday constant (96485 C mol^{-1}), R is the universal gas constant (8,314 J/mol·K), T is the absolute temperature (K), p_{O_2} is the measured oxygen partial pressure, ΔG is the free enthalpy of the reference electrode and z is the number of charges transported by the electrolyte per mole of oxygen [9,14]. According to the relation (2):

$$\underset{\text{gas}}{O_2} + 4e^- \underset{\text{electrode}}{\Leftrightarrow} \underset{\text{ionconductor}}{2O^{2-}}, \tag{2}$$

four charges are transported per mole of oxygen, $z = 4$ [14]. In case of the nickel/nickel oxide mixture used for the reference electrode, the following value for the free enthalpy was experimentally obtained [14]:

$$\Delta G = -474047.2 + 173.636 \cdot T \quad \text{(J)}. \tag{3}$$

Equation (1) and (3) will be used to calculate theoretical dependences (see Figs. 7 and 9).

3. Experimental

Four structures of potentiometric oxygen sensors have been fabricated and investigated. The structures were constructed from the following materials. The electrolyte was in the form of a pellet of about 1 cm in diameter, 100 μm thick (structure A, C, D) and 2 mm thick (structure B) yttria-stabilized zirconia (YSZ, chemical formula $Zr_{0.84}Y_{0.16}O_{2-x}$). The former was prepared from tape YSZ, while the later by compacting the YSZ powder (Tosoh, Japan). In both cases the green YSZ was sintered at 1400 ºC to obtain dense ceramics. Porous platinum films were prepared using platinum paste (ESL 5554) and brushing method on YSZ substrate structures A, C) or on NiO (structure B, D). The platinum electrodes were fired at 900 ºC for 1 hour to form porous adhered layers [14]. The NiO films were deposited on YSZ substrate (structure B, D) or on YSZ substrate with platinum electrodes (structures A, C) using nickel paste and brushing method. YSZ substrates with NiO were fired at 1250 ºC for 1 hour. In case of structures A and C, the Pt electrode, initially fired at 900 ºC, was finally annealed at 1250 ºC due to a co-firing process with Ni electrode. The initial firing of the Pt electrode at 900 ºC has provided a porous Pt structure, which after co-firing with a Ni electrode helped to obtain a strong interface of interconnected Pt and Ni particles. In order to obtain the electrical connection to the electrodes, thin Pt or Au wires were attached using Pt paste to the Pt electrode at the time of preparation of the Pt electrode.

To avoid re-oxidation of nickel, the reference electrode is sealed from ambient air using ESL 4909 glass sealing (structures A, B, C) or ESL 4905 (structure D). The glass has been in direct contact with the reference electrode in case of structures A and B, while this contact was avoided in case of structures C and D. In the former case the paste ELS 4909 was deposited on the reference electrode (thickness of about 60 μm), while in the latter case a plate of alumina was used to cover the reference electrode and the glass was used only on the

edges between alumina and YSZ. The paste ESL 4909 was used in the case of structure C, while the ESL 4905 in the case of structure D. In each case the glass paste was annealed at 900 ºC for 1 hour. Fig. 2 presents all schemes of the fabricated structures.

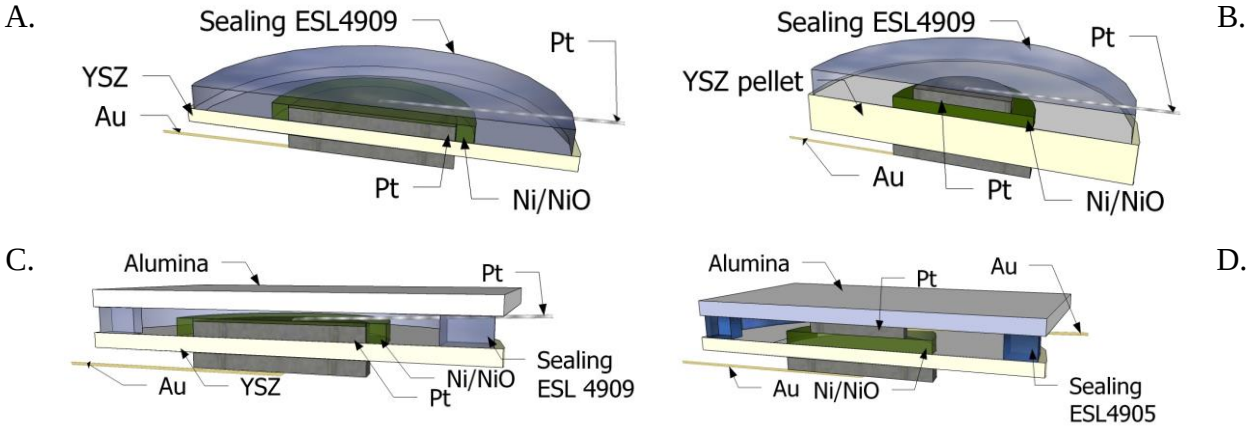

Fig. 2. Schematic diagrams of the prepared structures.

A key feature of this sensor is the internal oxygen reference electrode made of a suitable metal-metal oxide mixture having sufficient electric conductivity [15]. After sealing the nickel is in a fully oxidized form. To obtain a metal-metal oxide mixture the nickel oxide was in situ electrochemically reduced using an Electrochemical Interface SI1287. In order to measure open circuit potentials, the structures were placed at the centre of a tube furnace and connected to the SI1287 using platinum leads.

The furnace thermocouple was placed at a distance of about 1 cm from the investigated structures inside the test chamber. Therefore, the structure temperature was assumed as the set point of the furnace. The sensor was operated at 700 °C, which is sufficient to obtain satisfactory oxygen ion conductivity of the electrolyte and fast electrode kinetics [16]. The electrochemical formation of nickel was conducted at 700 ºC, which seems to be low enough to avoid alloy formation between Pt and Ni and pump oxygen relatively fast for NiO reduction [6, 8]. Upon thermal stabilization the structure was polarized with 1.4 V for 5 hours (the NiO electrode at negative terminal, while the counter Pt electrode at positive terminal). After polarization, the open circuit potential was measured for 1 hour in order to monitor the voltage and its stability. The structures before and after polarization experiments were investigated by impedance spectroscopy. For this purpose an impedance analyzer SI1260 was employed. The measurements were conducted in the frequency range 1 Hz – 1 MHz with an excitation signal of 20 mV. The procedure of polarization, open circuit voltage and impedance measurements were repeated 3 more times before any other measurements were carried out.

Different oxygen concentrations were obtained by mixing synthetic air and premixed concentration of 1%, 100 ppm and 1 ppm oxygen in nitrogen (cylinders from Linde Gas). The desired concentrations were achieved using mass flow controllers (Tylan GmbH). The total flow of gas mixtures in the measurement chamber was always set to 100 sccm.

It is worth mentioning that a structure consisting of paste ESL4905 in direct contact with the reference electrode was tested. However, it was not possible to obtain any voltage after the electrochemical reduction of nickel oxide. Most likely, a reaction between the nickel/nickel oxide and the ESL4905 occurred, with block formation of the chemical potential. This phenomenon was not investigated in detail and is therefore not presented in this paper.

4. Results and discussion

4.1. In situ chemical potential of reference electrode formation

The pictures of prepared structures are shown in Fig. 3. During examination of the structures it can be seen that, in case of structure A, there are cracks in the sealing glass (barely visible), while in the case of structures C and D there are cracks in the electrolyte. This effect is not related to the synthesis, since the cracks were not observed after the synthesis process and were noticed after the measurements. The mixture of nickel-nickel oxide from nickel oxide was formed *in situ* by polarization of the structure at 1.4 V for 15 hours (3 cycles of 5 hours) at 700ºC. Fig. 4 shows the currents as a function of time during the first 5 hours of the polarization process. The plot shows that structure C and D reveal significantly larger current levels than the structures A and B. This may suggest that the reference electrode is not properly sealed from the ambient atmosphere. Indeed, once the open circuit voltage was monitored after the polarization process at 700ºC, the measured voltage quickly reached about 0 V. It seems that the cracks in the electrolyte, visible in Fig.3, were formed during the polarization process of the reference electrode. For these structures the electrolyte was relatively thin (100 μm). Moreover, the structures C and D have embodied dead volumes between the electrolyte and alumina cover which are filled with air. The oxygen entrapped in these dead volumes is removed during the polarization process, what leads to significant pressure changes in the cavity. This process may cause the electrolyte to crack. Therefore, it seems that any dead volumes in the sensor structure should be avoided or the sealing process should be performed in an inert gas (i.e. nitrogen).

The measurements of the open circuit voltage show that for the structures A and B the voltages are close to the theoretical value. After polarization an open circuit potential of about 750 mV was obtained, which is comparable with the literature data of 760 mV [13]. The electric current levels for the structures A and B are not significantly different. In case of structure A the current level at the beginning of reduction is lower than in case of structure B. With time, in case of the structure A, the current starts to increase and finally is slightly higher than for structure B. This can be explained by the design differences. In case of structure B the low-conductivity nickel oxide is between the platinum electrode and YSZ, while in the case of structure A the platinum electrode is in contact with YSZ. Apparently, the reduction process of oxygen starts to be more effective once the nickel oxide is reduced in the vicinity of platinum (structure A), while for the nickel electrode relatively constant (structure B). It can be concluded that the level of the current during in situ formation of the reference electrode is very important. Too high current informs of leakage in the reference electrode sealing.

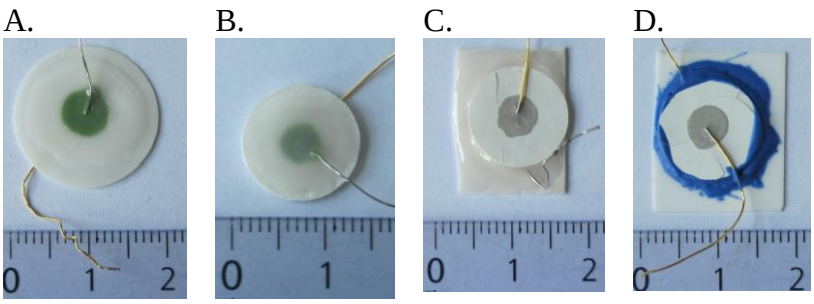

Fig. 3. Pictures of the prepared structures.

In Fig. 5 all three cycles of reference electrode reduction process for the structure A are presented. Both current and voltage are shown. Based on the Faraday law and the electric change passed during the reduction process one can calculate the amount of the NiO reduced. In case of structure A, it was calculated that after 15 hours of reduction the mass ratio Ni:NiO is 5%:95%, while in the case of structure B it is 2%:98%. In case of the structures C and D more oxygen was pumped than available in NiO. This confirms that the sealing of the structures C and D is not effective and additional ambient oxygen is pumped. In case of the structures with properly sealed reference electrode in each cycle about the same charge has passed and during a 5-hour reduction at 1.4 V less than 3% of NiO can be reduced.

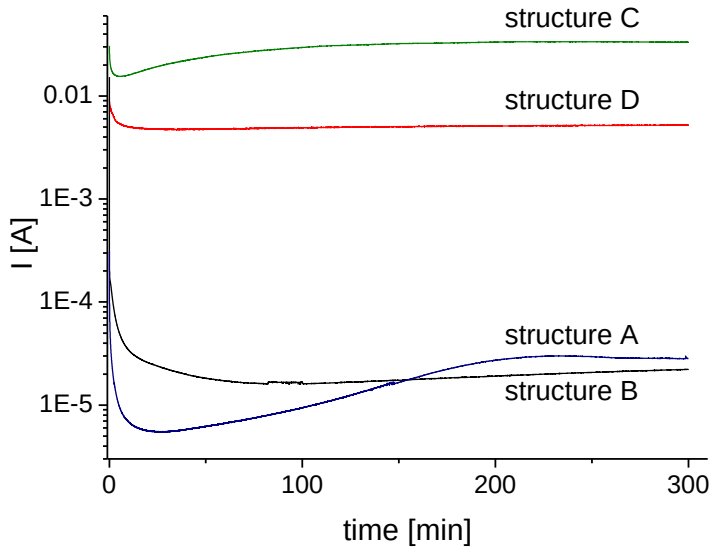

Fig. 4. The current during *in-situ* reference electrode formation for various structures (first cycle).

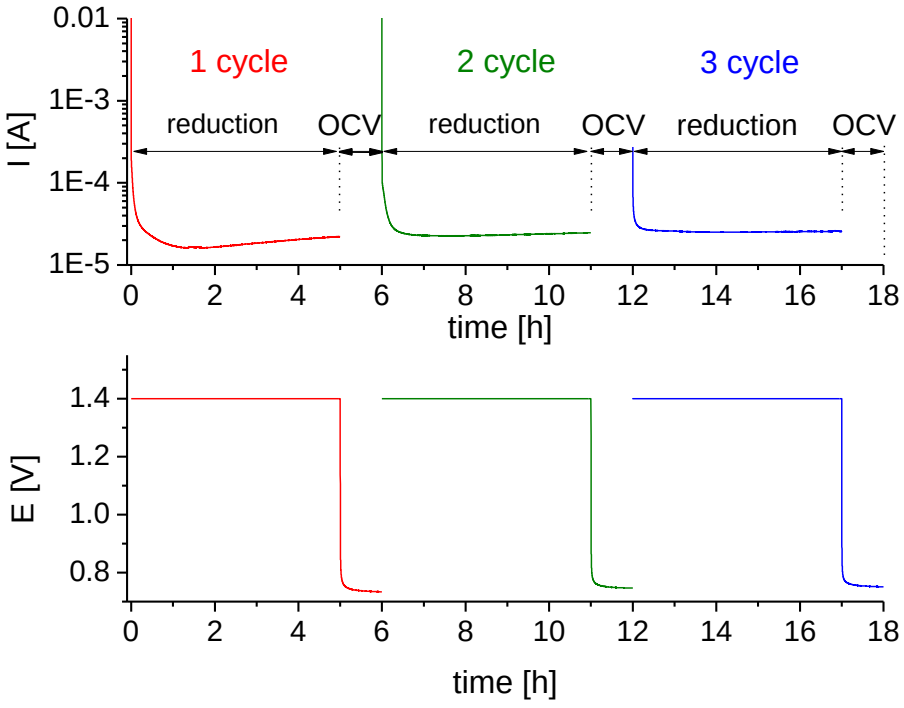

Fig. 5. The current and voltage plots as a function of time during *in-situ* reference electrode formation and open circuit voltage (OCV) for the A structure (all 3 cycles).

Valuable information can be obtained from the impedance spectra. Fig. 6 presents the modulus of impedance for the structures A and B before and after the polarization process. It can be seen that the impedance at high frequency (>10 kHz) is about an order of magnitude higher for structure B than for structure A. The high frequency impedance can be attributed to ohmic resistance of the structure, which is mostly related to the electrolyte thickness.

At low frequencies (<10 Hz) the impedance can be attributed to the efficiency of oxygen redox electrode process. It can be seen that the impedance for structures A and B before reduction is different. Namely, the impedance of structure B is higher than that for structure A, what can be explained by the difference in the design. For structure A the electrode is made of platinum, which is known to be a very good catalyst for oxygen reduction. In case of the B structure the electrode is made of nickel/nickel oxide, which for oxygen reduction is performing slightly worse than platinum [13]. This can also explain the lower currents during polarization for the structure B in comparison with structure A (see Fig. 4). Actually, based on the polarization voltage and the polarization current one can estimate the DC total resistance of the sensor during the polarization process. It was calculated that in case of structures A, B and D the total resistance was estimated to be about 50 kΩ, 63 kΩ and 270 Ω, respectively. These resistances are very close to the values of the AC resistance at low frequencies, which were obtained in an open-circuit condition. Namely, in the case of structures A, B and D an AC resistance of about 20 kΩ, 50 kΩ and 500 Ω was recorded (see Fig. 6 and 7), respectively.

It can also be noted in Fig. 6 that the impedance at low frequencies for the sample after reduction is always higher than for the same samples before reduction. This is in agreement with the fact that the oxygen partial pressure in the reference chamber after reduction is lower than that before reduction. The low partial pressure at the reference electrode slows down the efficiency of oxygen red-ox electrode process.

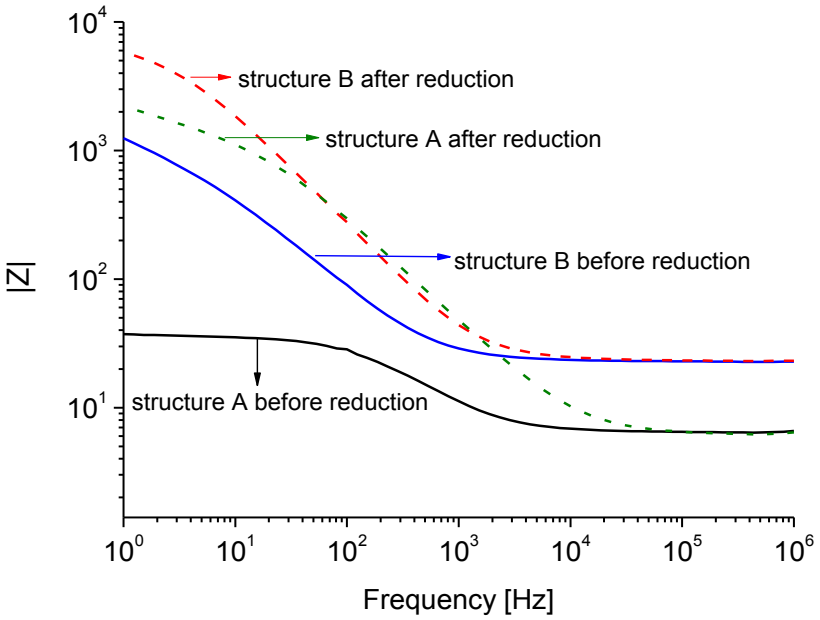

Fig. 6. The modulus of impedance for structure A and B before and after *in-situ* formation of nickel in the reference electrode.

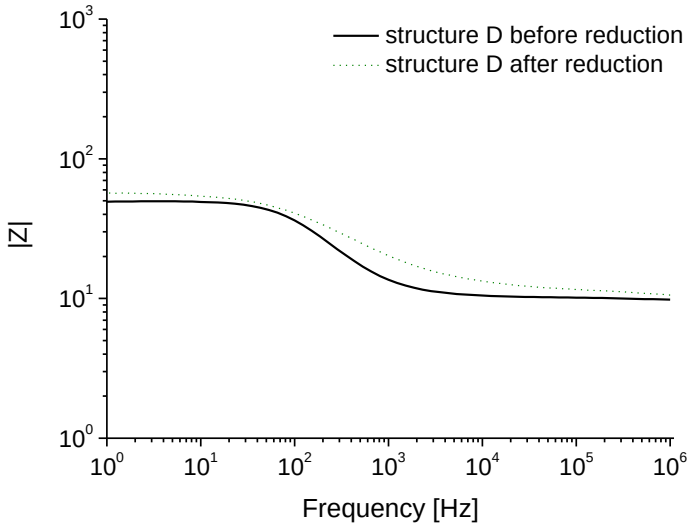

Fig. 7. The modulus of impedance for structure D before and after *in-situ* formation of nickel in the reference electrode.

Fig. 7 shows the modulus of impedance for structure D before and after reduction process. It can be seen that at low frequency (<10 Hz) the impedance is only insignificantly increased after the reduction process. Since oxygen leakage is expected, the oxygen partial pressure in the reference chamber after reduction might be only slightly lower and the efficiency of the redox process is about the same before and after the reduction process. The possible leakage sources were discussed by Kaneko et al.[17], Maskell [8] and Fouletier [18], however, in case of structure D it is evident that the leakage is due to the crack in the electrolyte.

Fig. 8 shows the EMF signal as a function of temperature showing the Nernstian behavior of the sensor B in the temperature range from 500 ºC to 700 ºC. The theoretical values were estimated based on the equations (1) and (3). It can be seen that whereas the slopes are identical, the EMF is slightly lower than the theoretical calculations. The cause of this difference is currently unknown. One reason for that difference could be the ratio of Ni:NiO after reduction, which after 15 hours of reduction is 5%:95%. Analyzing the open circuit voltage after 5 hours (0.733 V), after 10 hours (0.747 V) and after 15 hours (0.751 V) of reduction it can be noted that the OCV increases. Therefore, is it expected that open circuit voltage could be even larger once the ratio of Ni:NiO would be 50:50%.

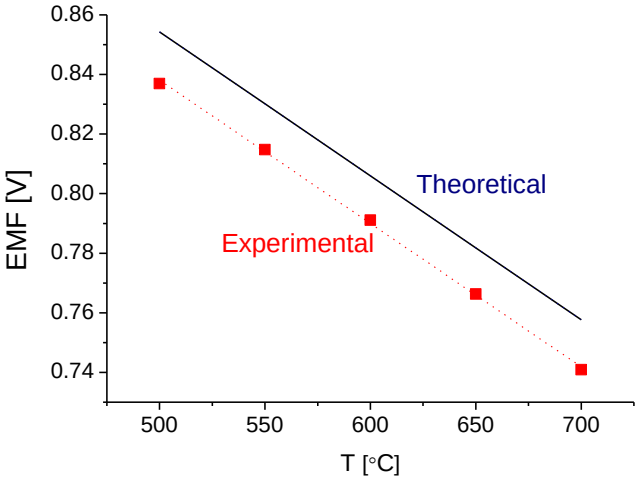

Fig. 8. Comparison of the theoretical and experimental data at different temperatures showing Nernstian behavior (sensor A).

4.2. Sensor response

Fig. 8 shows the response of sensor A for different oxygen concentrations at 700ºC. The response is reasonably fast considering the large volume of the testing chamber (about 1.2 dm^3). The response is below 120 s at this temperature. Results of Beie and Gnorich [19] confirm that this value may be attributed to gas exchange in the measurement chamber.

Fig. 9 shows the EMF signal as a function of oxygen concentration based on the response presented in Fig. 8. The sensor shows the Nernstian behavior, while the slope is practically identical for the experimental and theoretical data. The existing offset between the experimental and theoretical data is consistent with the difference in EMF difference presented in Fig. 7. A small change in the inclination angle visible at about 1% can be associated with the switching between different oxygen cylinders during the experiment. The calculated difference of about 6% was obtained in comparison with theoretical data, but in Chowdhury et al. a much greater difference of about 44% was reported [8].

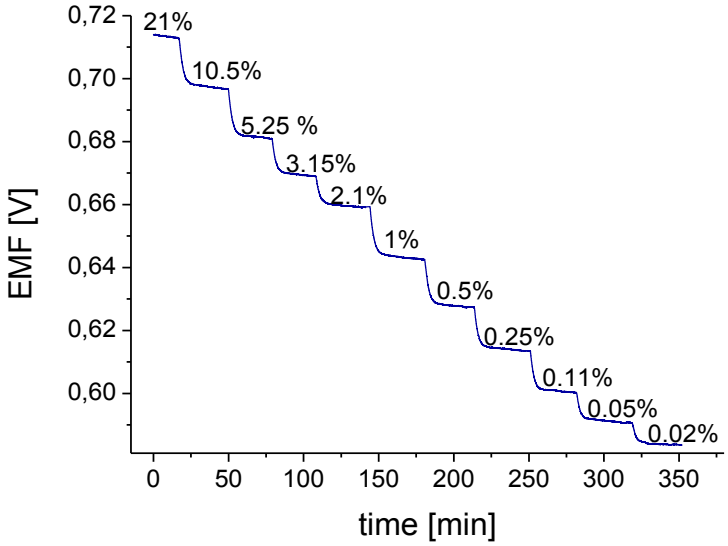

Fig. 8. Response characteristics of the sensor A at different oxygen concentrations at 700 ºC.

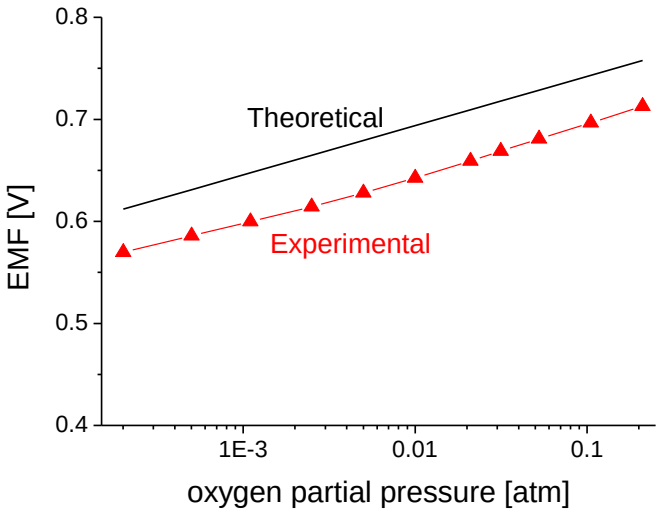

Fig. 9. Comparison of the theoretical and experimental data showing Nernstian behavior at 700 ºC (sensor A).

The response behavior of sensor A at 700 ºC is depicted in Fig. 10. It shows four cycles of switching between different oxygen levels (21% and 1%) in the chamber with each cycle lasting for about 1 hour. This response proves good sensor repeatability. The difference in voltage in each cycle (ΔE as depicted in Fig. 10) is a constant value of about 64 mV. However, after repeated tests over a longer period, the sensor performance degraded. A noticeable amount of drift was observed in the sensor signal, when the sensor was continuously tested at 700 ºC in air over 3.5 days. The drift might possibly arise due to grain growth and sintering of the inner electrode [8]. However, it might come from nickel oxidation due to small and barely visible cracks in the sealing glass. It seems that the relatively thin YSZ electrolyte (100 μm) is not appropriate for the potentiometric sensors with solid reference electrode. The pressure difference during the polarization process may result in the electrolyte mechanical deflection, what causes cracks in the electrolyte or in the glass. A thicker electrolyte may minimize the deflection.

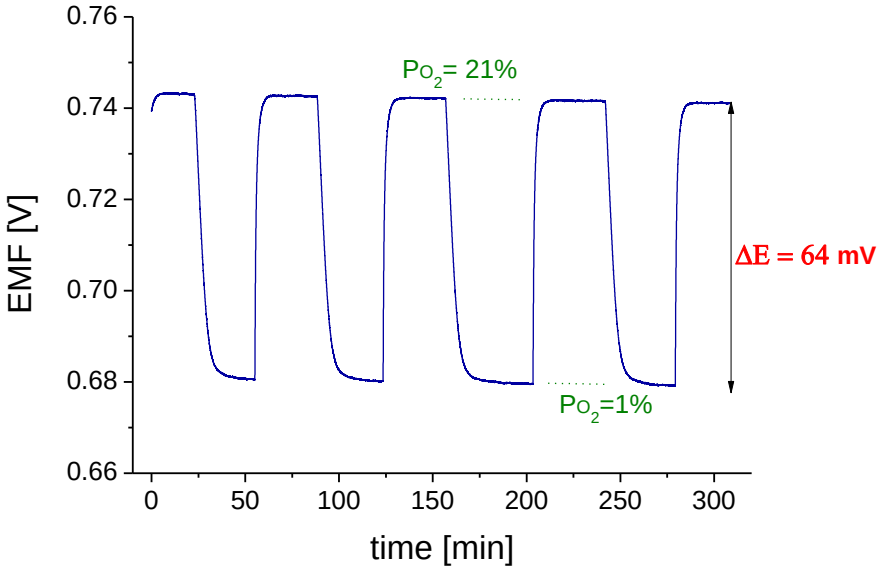

Fig. 10. Sensor A – transient response to 21% and 1% of oxygen.

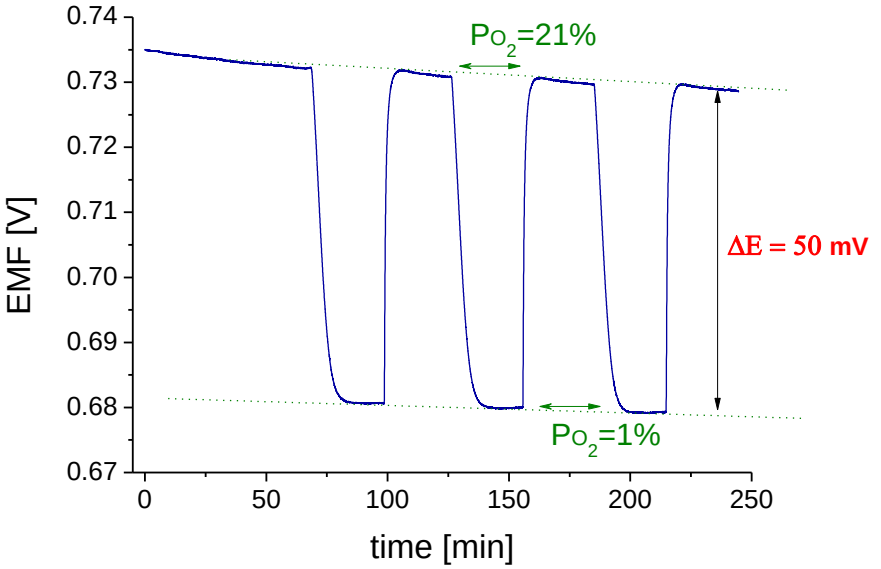

Fig. 11. Sensor B – transient response to 21% and 1% of oxygen.

The response behavior of sensor B at 700ºC was also tested and is depicted in Fig. 11, which shows three cycles of switching between oxygen concentration of 21% and 1%. The difference in voltage in each cycle is lower in comparison with structure A and is about 50 mV. Moreover, a noticeable amount of drift was observed in the sensor signal, whose cause is not evident. It is believed that the drift might be due to diffusion of oxygen within the reference electrode. Since the reduction process was relatively slow, it is believed that the stoichiometry of oxygen across the thickness of nickel/nickel oxide reference electrode is not uniform. These phenomena need to be investigated in detail to draw further conclusions.

4. Conclusions

In this paper different structures of oxygen sensors with a solid state reference nickel/nickel oxide electrode were fabricated and evaluated. Impedance spectroscopy was employed to investigate the effectiveness of the reduction process and the sealing of the reference electrode. The measurements show that the structures with dead volume in the vicinity of the reference electrode and a relatively thin electrolyte were not advantageous. During the polarization process significant changes in the pressure caused cracking of the electrolyte. The most promising was the structure with nickel oxide separated from the electrolyte by a platinum layer and without dead cavities. In this case the response was Nernstian and reproducible. However, the sensor was successfully working only a few days due to some cracks in the sealing glass. It is believed that the cracks propagated during the polarization process as a result of electrolyte mechanical deflection. Nevertheless, the preliminary study provided significant understanding in the fabrication needs of the potentiometric sensor with a solid state reference electrode.

Acknowledgements

The work was supported by the National Centre for Research and Development, LIDER No. 22/103/L-2/10/NCBiR/2011 „Multisensor system for measuring air pollutants”.

References

[1] Szabo, N., Lee, C., Trimboli, J., Figueroa, O., Ramamoorthy, R., Midlam-Mohler, S., Soliman, A., Verweij, H., Dutta, P., Akbar, S. (2003). Ceramic-based chemical sensors, probes and field-tests in automobile engines. J. Materials Science, 38, 4239–4245.

[2] Akbar, S., Dutta, P., LeeHigh, C. (2006). Temperature Ceramic Gas Sensors: A Review. Int. J. Appl. Ceram. Technol., 3 (4) 302–311.

[3] Kotarski, M., Smulko, J. (2009). Noise measurement set-ups for fluctuations-enhanced gas sensing. Metrol. Meas. Syst, 16(3), 457−464.

[4] Kalinowski, P., Woźniak, Ł., Strzelczyk, A., Jasinski, P., Jasinski, G. (2013). Efficiency of Linear and Non-Linear Classifiers for Gas Identification from Electrocatalytic Gas Sensor. Metrol. Meas. Syst, 20(3), 501−512.

[5] Kaneko, H., Okamuraa, T., Taimatsu, H., Matsuki, Y., Nishida, H. (2005). Performance of a miniature zirconia oxygen sensor with a Pd–PdO internal reference. Sensor Actuat. B-Chem. 108, 331–334.

[6] Radhakrishnan, R., Virkar, A. V., Singhal, S. C., Dunham, G. C., Marina, O. A. (2005). Design, fabrication and characterization of a miniaturized series-connected potentiometric oxygen sensor. Sensor Actuat. B-Chem., 105, 312−321.

[7] Sprig, J. V., Ramamoorthy, R., Akbar, S. A., Routbort, J. L., Singh, D., Dutta, P. K. (2007). High temperature zirconia oxygen sensor with sealed metal/metal oxide internal reference. Sensor Actuat. B-Chem., 124, 192−201.

[8] Chowdhury, A. K. M. S., Akbar, S. A., Kapileshwar, S., Schorr, J. R. (2001). A Rugged Oxygen Gas Sensor with Solid Reference for High Temperature Applications. J. Electrochem. Soc., 148, G91−G94.

[9] Maskell, W. C., Steele, B. C. H. (1986). Solid state potentiometric oxygen gas sensors. J. Appl. Electrochem., 16, 475−489.

[10] Maskell, W. C. (2000). Progress in the development of zirconia gas sensors. Solid State Ionics, 134, 43−50.

[11] Jasiński, P. (2006). Solid-state electrochemical gas sensors. Materials Science Poland, 24(1), 269−278.

[12] López-Gándara, C., Ramos, F. M., Cirera, A. (2009). YSZ-Based Oxygen Sensors and the Use of Nanomaterials: A Review from Classical Models to Current Trends. Journal of Sensors, 2009, 258489.

[13] Hu, Q., Jacobsen, T., Hansen, K. V., Mogensen, M. (2012). Improved Internal Reference Oxygen Sensors with Composite Ceramic Electrodes. J. Electrochem. Soc., 159, B811−B817.

[14] Vollath, D. (1976). A Non-Destructive Method for Determining the Oxygen/Metal Ratio in Plutonium-Bearing Nuclear Oxide Fuel. Proceedings of a Seminar on Nuclear Fuel Quality Assurance Held by the International Atomic Energy Agency in Oslo, 165−173.

[15] van Setten, E., Gür, T. M., Blank, D. H. A., Bravman, J. C., Beasley, M. R. (2002). Miniature Nernstian oxygen sensor for deposition and growth environments. Rev. Sci. Instrum., 73, 156−161.

[16] ChaoYang, X., Xu Chen, L., Yan, Y., Ti Zhuang, W., Zhi Min, Z., Su Ping, Y. (2011). Preparation of nano-structured Pt–YSZ composite and its application in oxygen potentiometric sensor. Applied Surface Science 257, 7952−7958.

[17] Benammar, M., Maskell, W. C. (1993). A Novel Miniature Zirconia Gas Sensor with Pseudo-Reference: Amperometric Operation Providing Unambiguous Determination of Air-to-Fuel Ratio. Applied Physics A, 57, 45−50.

[18] Fouletier, J., Vitter, G., Kleitz, M. (1975). Measurement and regulation of oxygen content in gases using solid electrolyte cells. III. Oxygen pump-gauge. J. Appl. Electrochem., 5, 111−120.

[19] Beie, H. J., Gnorich, A. (1991). Oxygen gas sensors based on CeO2 thin film. Sensor Actuat. B-Chem., 4, 393−399.